Int J Adv Manuf Technol (2017) 93:35–41
DOI 10.1007/s00170-015-7636-7

ORIGINAL ARTICLE

# Optimization of flux-cored arc welding process parameters by using genetic algorithm

**B. Senthilkumar**[1] · **T. Kannan**[2] · **R. Madesh**[3]

Received: 21 February 2015 / Accepted: 21 July 2015 / Published online: 21 August 2015


**Abstract** The effect of flux-cored arc welding (FCAW) process parameters on the quality of the super duplex stainless steel (SDSS) claddings can be studied using Taguchi L9 design of experiments. In this experimental investigation, deposits were made with 30 % bead overlap. Establishing the optimum combination of process parameters is required to ensure better bead geometry and desired properties. The above objectives can be achieved by identifying the significant input process parameters as input to the mathematical models like welding voltage ($X_1$), wire feed rate ($X_2$), welding speed ($X_3$), and nozzle-to-plate distance ($X_4$). The identified responses governing the bead geometry are bead width ($W$) and height of the reinforcement ($H$). The mathematical models were constructed using the data collected from the experiments based on Taguchi L9 orthogonal array. Then, the responses were optimized using non-traditional nature-inspired technique like genetic algorithm (GA).

**Keywords** Bead geometry · Claddings · Flux-cored arc welding · Genetic algorithm · Pareto front · Super duplex stainless steel · Taguchi

✉ B. Senthilkumar
bsk_senthilkumar@hotmail.com

T. Kannan
kannan_kct@yahoo.com

R. Madesh
madeshspark@gmail.com

[1] Department of Mechanical Engineering, Kumaraguru College of Technology, Coimbatore 641 049, India

[2] Department of Mechanical Engineering, SVS College of Engineering, Coimbatore 642 109, India

[3] Department of Mechanical Engineering, Sri Guru Institute of Technology, Coimbatore 641 110, India

## 1 Introduction

Cladding is the process of surfacing the low carbon steel substrate with corrosion-resistant materials like stainless steels. The advantages of claddings over conventional bulk stainless steel structures are low cost, ease of fabrication, and serviceability. Performance of the surfaced layer in the aggressive environments can be improved by depositing super duplex stainless steel [1–3]. Duplex stainless steel has equal proportions of austenite and ferrite content on the microstructure. The increased alloy content is responsible for its high strength and corrosion resistance [5]. Stainless steel claddings can be produced by various methods like roll bonding, welding, and explosive cladding. Welding has the ability to process prefabricated components along with ability to control dilution and bead geometry. The availability of different welding processes to meet the industrial demands like deposition rate, portability, positional welding and automation capabilities. Flux-cored arc welding (FCAW) process was used in this experimental investigation because of its smooth bead surface, high deposition rate, and easy slag removal [4]. The selection of welding process parameters plays a significant role in determining the bead geometry and surface quality [5].The properties of the super duplex stainless steels are sensitive to welding heat input, and it is limited between 0.5 and 1.5 kJ/mm; this constraint limits the deposition rate within in a narrow range [6, 7]. Any attempt to increase bead geometry increases heat input leading to precipitation complex intermetallic phases which reduce the strength and corrosion resistance. The objective of any surfacing process is to maximize the reinforcement geometry with desired heat input and joint strength. The relationship between the welding process parameters and the bead geometry can be modeled using either mathematical or brain-inspired neural networks. Mathematical models can be used to explore the influence of welding process parameters on the bead geometry variables [8].

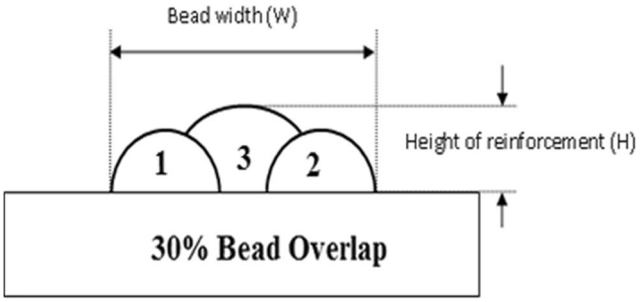


**Fig. 1** Bead geometry

The use of designed experiments facilitates construction of models using minimum number of experimental runs without sacrificing the prediction accuracy of the models [9]. The objective of using the Taguchi's L9 orthogonal array is to minimize the variance in the responses for all combination of welding process parameters [10]. Taguchi techniques can be effectively used in the optimization of multiple objectives using gray relational analysis [11]. The developed models can be used to perform the simulation, optimization, and evaluation of sensitivity of the welding parameters [12]. Regulation and optimization of the bead geometry reduce the number of welding passes required to cover the given surface area [13, 14]. Figure 1 shows sequence of deposition adopted in this work and measurement of bead geometry variables like bead width ($W$) and reinforcement height ($H$). Genetic algorithm is inspired by Darwin's theory of biological evolution and has been recognized as a general optimization method to produce global and robust solutions to optimization problems [15]. Genetic algorithm was preferred because of its ability to handle multi-dimensional problems with multiple solutions. The concept of Pareto frontier was implemented to achieve the trade-off between the two objective functions are bead width and reinforcement height [16]. The use of genetic algorithm in the optimization of bead geometry in welding leads to faster convergence to the global optimum values [17–19]. The objective of this experimental investigation is to model and optimize the reinforcement dimensions in the multi-pass super duplex stainless steel (2507) claddings deposited by FCAW process. The process parameters used in the study was welding voltage ($X_1$), wire feed rate ($X_2$), welding speed ($X_3$), and nozzle-to-plate distance ($X_4$). The responses measured are reinforcement height ($H$) and bead width ($W$). The ferrite content of the deposits was measured using Ferritescope MP30 calibrated according to the ANSI/AWS A4.2 standard. The first-order regression models were combined into a single objective function for the optimization using genetic algorithm. The development of Pareto frontier enables the process designer to select from the group of alternatives to meet the needs of the industry. After the development of regression models, genetic algorithm was used to identify non-dominated solutions in the parameter space.

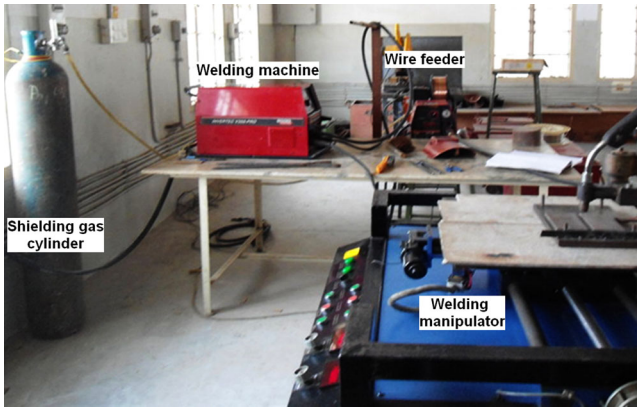


**Fig. 2** Experimental setup

## 2 Experimental investigation

The experimental setup consists of multi-process welding machine Lincoln Electric® Invertec® V350 pro coupled with wire feeder LF-74. The electrode was a 1.2-mm-diameter Metrode™ Supercore™ FC2507 (AWS A5.22E2594T0-4) and base plate is IS:2602 low carbon structural steel. Table 1 presents the composition of the electrode and base metal. The shielding gas mixture contains 80 % Argon and 20 % $CO_2$ supplied at a rate of 24 l/min. Figure 2 shows the experimental setup. The steps involved in this work regarding the data collection, model development, and optimization were categorized as follows:

Step 1: Identification of process parameters and responses
Step 2: Finding the limits and levels of process parameters
Step 3: Construction of design matrix
Step 4: Experimental work and data collection
Step 5: Development of mathematical models
Step 6: Optimization of the process parameters

**Table 1** Composition of electrode and base metal

| Material | Elements (%wt) | | | | | | | | | | |
|---|---|---|---|---|---|---|---|---|---|---|---|
| | C | Mn | Si | S | P | Cr | Ni | Mo | Cu | N | Fe |
| Electrode | 0.027 | 0.64 | 0.47 | 0.005 | 0.018 | 25.8 | 8.62 | 4.36 | 0.06 | 0.28 | Balance |
| Base metal | 0.196 | 1.12 | 0.293 | 0.011 | 0.0044 | 0.128 | 0.0336 | 0.0275 | 0.0963 | – | Balance |

**Table 2** Process parameter levels and coding

| S. no | Parameters | Symbol | Units | Factor levels | | |
|---|---|---|---|---|---|---|
| | | | | 1 | 2 | 3 |
| 1. | Welding voltage | $X_1$ | V | 22 | 26 | 30 |
| 2. | Wire feed rate | $X_2$ | m/min | 5.08 | 6.35 | 7.62 |
| 3. | Welding speed | $X_3$ | m/min | 0.12 | 0.16 | 0.20 |
| 4. | Nozzle to plate distance | $X_4$ | m | 0.015 | 0.019 | 0.023 |

### 2.1 Identification of process parameters and responses

The selection of welding process parameters for this investigation was based on their influence on heat input. The welding voltage has direct influence on heat released and arc width at the base metal. The parameter wire feed rate has control on welding current, metal transfer characteristics, and electrode melting rate. The bead dimension was closely associated with torch travel speed, otherwise welding speed. Nozzle-to-plate distance influences the distribution of heat between the electrode and base metal. It also influences the resistance heating of the electrode and effectiveness of the shielding gas on the weld puddle.

### 2.2 Finding the limits and levels of process parameters

The experiments were conducted at the welding research center in Kumaraguru College of Technology, Coimbatore, India. The range of process parameters was established by conducting trial runs, and the deposits were visually inspected. In the absence of defects like cracking, porosity, and discontinuity, the maximum value was coded as 3 and minimum value was coded as 1. The same procedure was followed for the remaining variables. Table 2 presents the levels and its corresponding actual values of the process parameters.

### 2.3 Construction of design matrix

The experimental data required to relate the FCAW process parameters with responses were collected using the Taguchi L9 orthogonal array. The design matrix consists of nine experimental runs. The experimental parameter combinations with measured responses like bead width, reinforcement height, and ferrite number are presented in the Table 3.

### 2.4 Experimental work and data collection

The welding voltage is set at the welding machine, and wire feed rate is controlled at the wire feeder. The parameters like welding speed and nozzle-to-plate distance were set at the manipulator. The base plate was moved against the stationary welding torch. The base plate was cleaned thoroughly to remove any oxide layer and residues using the finest-grade sand paper. The plates were allowed to cool to room temperature after depositing each weld bead. The bead width and reinforcement height measurements were taken at the first deposit to calculate the centerline for the next deposit. The percentage overlap was fixed at 30 % between the weld beads. The experimental combinations were selected from Table 3 at random, to introduce variance in the experimental settings error. The measured bead geometry data like reinforcement height ($H$) and bead width ($W$) are presented in Table 3. The weld bead was sectioned and polished. Figure 3 shows the sectioned weld bead for the experimental runs 4 and 9 prepared for the bead geometry measurement. The third deposit is well connected with first and second deposit, but lack of fusion

**Table 3** Design matrix with measured responses

| Ex. No. | Process parameters (un-coded) | | | | Responses | | Average ferrite number (measured) |
|---|---|---|---|---|---|---|---|
| | Welding voltage ($X_1$) V | Wire feed rate ($X_2$) m/min | Welding speed ($X_3$) m/min | Nozzle to plate distance ($X_4$) m | Bead width ($W$) mm | Reinforcement height ($H$) mm | |
| 1 | 22 | 5.08 | 0.12 | 0.015 | 21.63 | 5.60 | 27.89 |
| 2 | 22 | 6.35 | 0.16 | 0.019 | 17.46 | 6.53 | 29.6 |
| 3 | 22 | 7.62 | 0.20 | 0.023 | 16.70 | 7.13 | 25.57 |
| 4 | 26 | 5.08 | 0.16 | 0.023 | 19.70 | 5.42 | 27.93 |
| 5 | 26 | 6.35 | 0.20 | 0.015 | 22.46 | 4.98 | 30.47 |
| 6 | 26 | 7.62 | 0.12 | 0.019 | 27.64 | 7.08 | 29.08 |
| 7 | 30 | 5.08 | 0.20 | 0.019 | 18.11 | 4.29 | 28.32 |
| 8 | 30 | 6.35 | 0.12 | 0.023 | 26.43 | 6.18 | 28.66 |
| 9 | 30 | 7.62 | 0.16 | 0.015 | 29.17 | 5.06 | 28.8 |

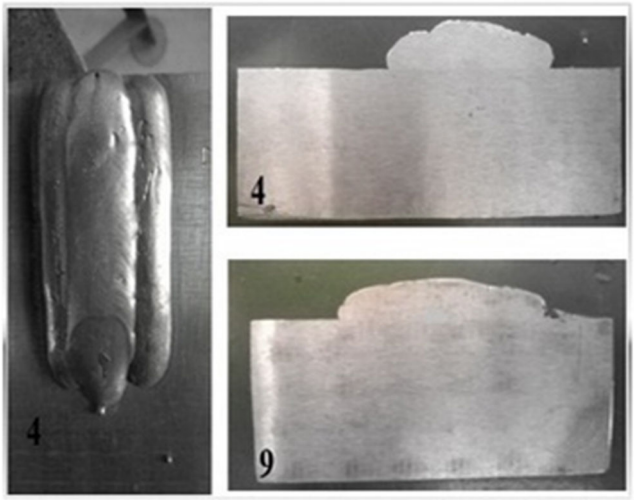


**Fig. 3** Sectioned specimens

with the substrate was observed. The top surface of the weld beads were ground and polished for the ferrite content measurement. The ferrite content of the deposits was found between 25.57 and 30.47. This is because rapid cooling of weld bead reduced the ferrite content in the deposits.

### 2.5 Development of mathematical models

The responses were presented as functions with the process parameters as its components, and it is given by the Eq. (1). The regression procedure was used for the development of mathematical model to optimize the bead geometry like bead width and reinforcement height:

$$\text{Responses } R = f(X_1, X_2, X_3, X_4) \quad (1)$$

where $X_1$, $X_2$, $X_3$, and $X_4$ are the welding voltage, wire feed rate, welding speed, and nozzle-to-plate distance, respectively.

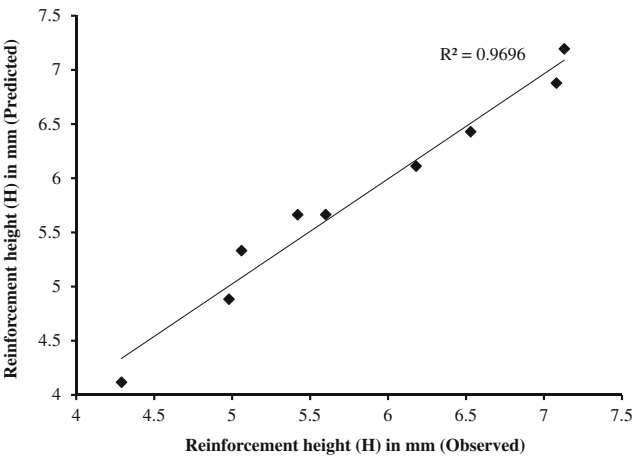


**Fig. 4** Scatter plot for reinforcement height

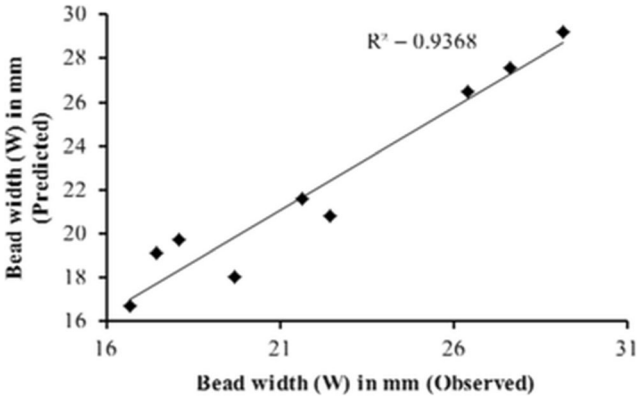


**Fig. 5** Scatter plot for bead width

The developed models for the prediction of reinforcement height and bead width are presented by the Eqs. (2) and (3):

$$W = 11.53 + 0.747_1 + 0.0469X_2 - 0.0768X_3 - 0.434X_4 \quad (2)$$

$$H = 5.75 - 0.156X_1 + 0.0132X_2 - 0.0102X_3 + 0.129X_4 \quad (3)$$

The validity of these models was tested by drawing scatter diagrams given by Figs. 4 and 5, which show the observed and predicted values of weld bead geometry.

### 2.6 Optimization of the process parameters

The electrode melting rate regulates the bead dimensions as well as heat input. The deposition rate has an extensive impact on the bead dimensions and dilution but does not affect the welding current. The main objective of weld cladding is to produce the desired bead dimension with low percentage dilution without affecting the bead integrity. To meet the above requirements, the objective function must be composed of both reinforcement height and bead width. Figure 4 presents that the Pareto front of the objective 1 is bead width and objective 2 is reinforcement height

## 3 Results and discussion

It has been found that the parameters wire feed rate and nozzle-to-plate distance have profound influence on the response reinforcement height than the others. The wire feed rate controls the welding current and the electrode melting rate. On the other hand, nozzle-to-plate distance has a

**Table 4** Model $R^2$ values

| Model | $R^2$ value | $R^2$ adjusted |
|---|---|---|
| Bead width ($W$) | 0.9368 | 0.8737 |
| Reinforcement height ($H$) | 0.9690 | 0.9380 |

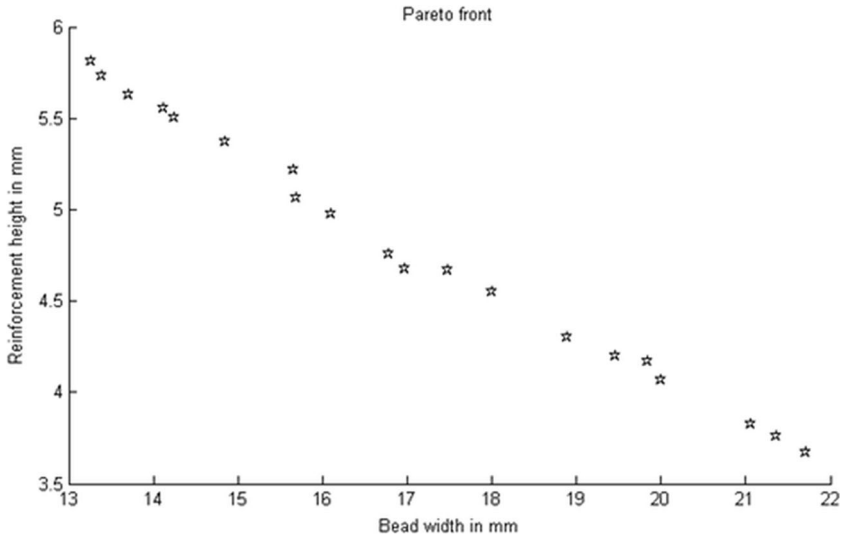


**Fig. 6** Pareto optimal for the responses reinforcement height ($H$) and bead width ($W$)

significant influence on the heat distribution on the weld puddle. The effect of arc current and arc pressure exhibits inverse relationship with the reinforcement height. From the experimental results, a mathematical model was developed using regression models.

Table 4 shows that the predictability of the models was well within the acceptable limits. These models can be used for the prediction as well as in the optimization of bead geometry.

The validity of these models was tested by drawing scatter diagrams given by Figs. 4 and 5, which show the observed and predicted values of weld bead geometry.

The responses bead width and reinforcement height were influenced by the welding voltage and nozzle-to-plate

**Table 5** Pareto optimal points

| Sl. no | Process parameters | | | | Responses | |
|---|---|---|---|---|---|---|
| | Welding voltage ($X_1$) V | Wire feed rate ($X_2$) m/min | Welding speed ($X_3$) m/min | Nozzle-to-plate distance ($X_4$) m | Bead width ($W$) mm | Reinforcement height ($H$) mm |
| 1 | 22.18 | 5.28 | 0.198 | 0.022 | 13.26 | 5.81 |
| 2 | 23.27 | 5.25 | 0.198 | 0.020 | 14.84 | 5.37 |
| 3 | 24.80 | 5.23 | 0.198 | 0.016 | 17.48 | 4.67 |
| 4 | 22.37 | 5.23 | 0.198 | 0.021 | 13.71 | 5.63 |
| 5 | 23.71 | 5.20 | 0.199 | 0.015 | 16.96 | 4.68 |
| 6 | 22.30 | 5.24 | 0.198 | 0.021 | 13.39 | 5.73 |
| 7 | 27.97 | 5.20 | 0.197 | 0.016 | 19.84 | 4.17 |
| 8 | 29.21 | 5.20 | 0.199 | 0.015 | 21.06 | 3.83 |
| 9 | 26.21 | 5.21 | 0.198 | 0.015 | 18.89 | 4.31 |
| 10 | 23.93 | 5.21 | 0.199 | 0.016 | 16.78 | 4.76 |
| 11 | 30.00 | 5.20 | 0.200 | 0.015 | 21.70 | 3.67 |
| 12 | 29.57 | 5.20 | 0.199 | 0.015 | 21.36 | 3.76 |
| 13 | 22.18 | 5.28 | 0.198 | 0.022 | 13.26 | 5.81 |
| 14 | 22.67 | 5.24 | 0.198 | 0.020 | 14.25 | 5.50 |
| 15 | 23.65 | 5.23 | 0.199 | 0.017 | 16.10 | 4.98 |
| 16 | 24.96 | 5.23 | 0.197 | 0.015 | 17.99 | 4.55 |
| 17 | 25.28 | 5.21 | 0.198 | 0.021 | 15.65 | 5.22 |
| 18 | 27.78 | 5.21 | 0.199 | 0.015 | 19.99 | 4.07 |
| 19 | 27.06 | 5.21 | 0.198 | 0.015 | 19.45 | 4.20 |
| 20 | 23.32 | 5.22 | 0.199 | 0.018 | 15.69 | 5.07 |
| 21 | 22.47 | 5.26 | 0.198 | 0.020 | 14.11 | 5.55 |

distance. The influence of these parameters on the arc width and arc pressure at the weld puddle can be exploited to produce the desired surface features in the minimum number of welding passes.

Figure 6 shows the Pareto optimal points generated from the optimization of bead width and reinforcement height. The response bead width was distributed between 13.26 and 21.7 mm. It is also observed that the reinforcement height was distributed between 3.67 and 5.81 mm. These optimal points present alternative solutions for the selection of layer thickness and minimization of the welding passes. Table 5 presents the parameter combinations for non-dominated Pareto optimal points. The details of the optimization environment were presented as follows"

GA settings
Population=60
Selection function=tournament
Crossover fraction=0.8
Crossover ratio=1.0
Distance measure function=distance crowding
Number of variables=4
Upper limit=[30, 300, 200, 23]
Lower limit=[22, 200, 120, 15]

## 4 Conclusion

In this experimental investigation, mathematical models were developed using four factors with three levels of Taguchi L9 orthogonal array used for the FCAW cladding process. The regression models were used for the multi-objective optimization using genetic algorithm on bead width and reinforcement height to identifying the most significant factors.

- The predicted results using mathematical models are very close to the experimental results as indicated by the scatter plots.
- Weld bead width and height of reinforcement increase with increase in wire feed rate. Weld bead width and height of reinforcement decrease with the increase in welding speed.
- The developed Pareto front presents number of non-dominated solutions in the parameters space.
- The result of the optimization shows the linear relationship between welding voltage with bead width and wire feed rate with reinforcement height.
- It is also observed that the higher values of nozzle-to-plate distance and welding speed favored buildup of reinforcement height.
- The low ferrite content of the deposits was due to low heat input to the surfacing process and rapid cooling.

The same models can be used for the weldment design with the objective of minimizing the reinforcement dimensions.

## References


1. Palani PK, Murugan N (2007) Development of mathematical models for prediction of weld bead geometry in cladding by FCAW. Int J Adv Manuf Technol 30:669–676
2. Bhatt RB, Kamat HS, Ghosal SK, De PK (1999) Influence of nitrogen in the shielding gas on corrosion resistance of duplex stainless steel welds. ASM Intrl JMEPEG 8:591–597
3. Palani PK, Murugan N (2007) optimization of weld bead geometry for stainless steel claddings deposited by FCAW. J Mater Process Technol 190:291–299
4. Vasanthakumar V, Murugan N (2011) Effect of FCAW process parameters on weld bead geometry in stainless steel cladding. J Miner Mater Charact Eng 10(9):827–842
5. Kannan T, Murugan N (2007) Effect of FCAW process parameters on duplex stainless steel clad quality. J Mater Process Technol 176: 230–239
6. Gomes JHG, Costa SC, Paiva AP, Balestrassi PP (2012) Mathematical modeling of weld bead geometry, quality, and productivity for stainless steel claddings deposited by FCAW. J Mater Eng Perform 21(9):1862–1872
7. Aloraier A, Almazrouee A, Shehata T, Price JWH (2012) Role of welding parameters using FCAW process of low alloy steels on bead geometry and mechanical properties. J Mater Eng Perform 21(4):540–547
8. Abbas E, Morteza S, Keyvan R (2012) Dilution and ferrite number prediction in pulsed current cladding of super duplex stainless steel using RSM. J Mater Eng Perform 10:677–685
9. Gunaraj V, Murugan N (1999) Application of response surface methodology for predicting weld bead quality in submerged arc welding of pipes. J Mater Process Technol 88: 266–275
10. Datta S, Asish B, Pradip Kumar P (2008) Application of Taguchi philosophy for parametric optimization of bead geometry and HAZ width in submerged arc welding using a mixture of fresh flux and fused flux. Int J Adv Manuf Technol 36(7–8):689–698
11. SundaravelVijayan RR, Rao SRK (2010) Multiobjective optimization of friction stir welding process parameters on aluminum alloy AA 5083 using Taguchi-based grey relation analysis. Mater Manuf Process 25(11):1206–1212
12. Arivazhagan B, Kamaraj M (2011) A study on factors influencing toughness of basic flux cored weld of modified 9Cr-1Mo steel. J Mater Eng Perform 20:1188–1195
13. Katherasan D, Elias JV, Sathiya P, Noorul Haq A (2012) FCAW parameters optimization using PSO algorithm. Procedia Eng 38: 3913–3926
14. Sudhakaran R, VelMurugan V, Sivasakthivel PS, Balaji M (2011) Prediction and optimization of depth of penetration for stainless steel GTAW plates using artificial neural networks and SA algorithm. Neural Comput Appl 22:637–649
15. Siva K, Murugan N, Logesh R (2009) Optimization of weld bead geometry in plasma transferred arc hardfaced austenitic stainless steel plates using genetic algorithm. Int J Adv Manuf Technol 41: 24–30
16. Torres-Trevino LM, Reyes-Valdes FA, Victor L (2011) Multi-objective optimization of a welding process by the

estimation of the Pareto optimal set. Expert Syst Appl 38: 8045–8053

17. Dey V, Kumar D, Datta GL, Jha MN, Saha TK, Bapat AV (2008) Optimization of bead geometry in electron beam welding using a Genetic Algorithm. J Mater Process Technol 9:1151–1157
18. Vasudevan M, Kuppuswamy MV, Bhaduri AK (2010) Optimising process parameters for gas tungsten arc welding of an austenitic stainless steel using genetic algorithm. Trans Indian Inst Met 63: 1–10
19. Dey V, Pratihar DK, Datta GL, Jha MN, Bapat AV (2009) Optimization and prediction of weldment profile in bead-on-plate welding of Al-1100 plates using electron beam. Int J Adv Manuf Technol 48:513–528